

Studies of Substorm on March 12, 1991: 2. Auroral Electrons. Acceleration, Injection, and Dynamics

L. L. Lazutin^a, T. V. Kozelova^b, N. P. Meredith^c, M. Danielides^d, B. V. Kozelov^b,
J. Jussila^d, and A. Korth^e

^a Skobel'tsyn Institute of Nuclear Physics, Moscow State University, Vorob'evy gory, Moscow, 119992 Russia
e-mail: lll@srd.snip.msu.ru

^b Polar Geophysical Institute, Kola Scientific Center, Russian Academy of Sciences, ul. Fersmana 14, Apatity, Murmansk oblast, 184200 Russia

^c British Antarctic Survey, Cambridge, Great Britain

^d Oulu University, Finland

^e Max Planck Institute, Lindau, Germany

Received April 13, 2005

Abstract—In the first part of this study of the substorm of March 12, 1991, the space-time structure of substorm disturbance and dynamics of auroral ions were considered. This second part presents an analysis of measurements of auroral electrons onboard the *CRRES* satellite. It is demonstrated that enhancements of the electron flux (injections) during large-scale and local dipolarizations of the magnetic field are determined by a combination of field-aligned, induction, and betatron mechanisms of acceleration with an effect of displacement of the drift shells of particles. The relative contributions of these mechanisms in relation to the energy of auroral electrons are determined.

PACS: 94.30.Lr, 94.30.Aa, 94.20.Ac

DOI: 10.1134/S0010952507020013

1. INTRODUCTION

Spectral and space-time characteristics of auroral electrons during substorms were studied in many papers (see, for example, [1] and references therein). The electron population in the magnetosphere is versatile in its energy characteristics, regions of habitation, and origin. One usually classifies as auroral electrons the populations of the magnetotail and of quasi-trapping regions that in the narrow sense bear relation to auroras, and in the broad sense they belong to substorm disturbances of different types.

In the zone of quasi-trapping, where the processes of the substorm studied by us are developed, auroral electrons are divisible into two groups: low energy (< 10 keV) and energetic (from ten up to a few hundred keV) electrons. The low energy electrons are usually referred to as plasma sheet electrons. In turn, they are divided in soft and hard electrons, the former being associated with the periphery or boundary plasma sheet and the latter with the central plasma sheet, respectively. The central plasma sheet (CPS) is usually considered as a part of the magnetotail plasma sheet, but in our opinion one should separate the CPS from the tail part both in its position inside the quasi-trapping region and in characteristics of the particles (electrons and ions) composing it. There are CPS electrons under quiet conditions as well, but during disturbances their fluxes are sharply intensified causing auroras. The intensifica-

tion is due to acceleration in field-aligned electric fields, the regions and mechanisms of acceleration are dynamic and diverse, as are diverse the forms of auroras. Energetic auroral electrons first discovered and studied with balloons and then onboard satellites appear in the auroral zone on the outer boundary of electrons of the radiation belt during strong disturbances, approximately coinciding (to an accuracy of minutes) with activations of auroras and with the appearance of field-aligned fluxes of low-energy electrons. The relationship of dynamics of these two species of auroral electrons is so far poorly studied and needs more precise investigations.

When a satellite, moving in the equator plane in the night quasi-trapping region, detects electrons with energies of 20–500 keV, one cannot distinguish an electron of the radiation belt from an auroral electron of the same energy. But these two populations of electrons are easily separable according to their energy spectra and space-time structures. The flux of electrons of the radiation belt decays monotonically when one moves away from the maximum of the outer belt, while the fluxes of auroral electrons are subject on this background to fast variations: they increase sharply and disappear either precipitating into the atmosphere or being spread in the process of magnetic drift and mixed with the radiation belt particles. Thus, auroral electrons represent a transient substance that exists only in a freshly accelerated form.

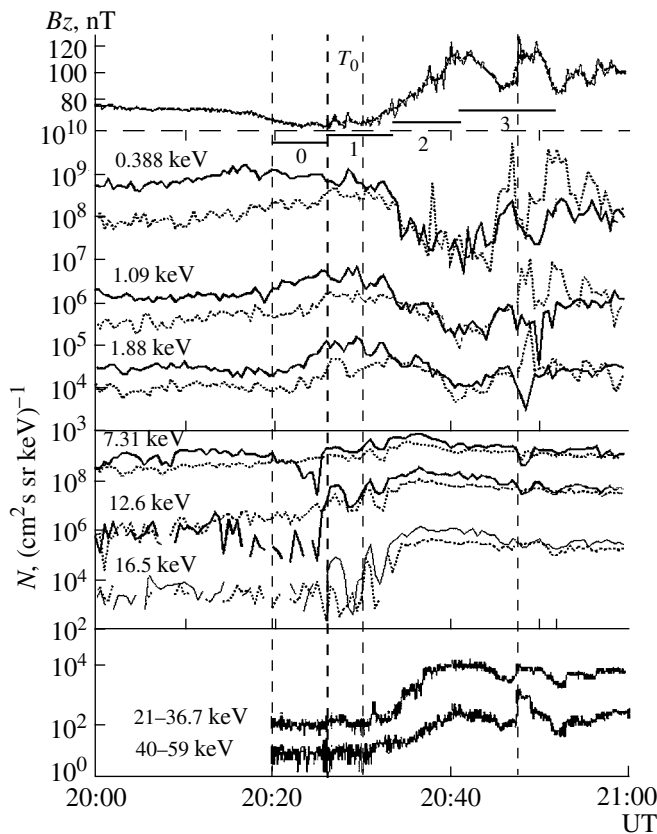


Fig. 1. B_z component of the magnetic field and electron fluxes measured by the *CRRES* satellite. Solid lines represent the fluxes of trapped electrons, and dotted curves show the fluxes along field lines. Vertical dashed lines mark the beginning of growth and active phases, as well as that of magnetic field dipolarization and local activation on the *CRRES* meridian.

Most frequently, acceleration of energetic electrons is explained by injection: particle transport takes place in the radial direction toward to the Earth from the tail into the region with stronger magnetic field and, accordingly, with betatron acceleration. The mechanism of acceleration by the induction field is equally popular. In addition, various mechanisms of acceleration in variable fields were suggested, for example, on the crest of a shock wave moving to the Earth. One can assume that basic mechanisms of acceleration of auroral particles are well known theoretically, but one cannot say that they are successfully brought into correlation with experimental data. The substorm activity is so multiform that observational material can be fit for confirmation of any theoretical concept. In this case, some simplifications are always made, and some facts remain that do not fall into a model pattern and are set aside as having minor importance.

In this paper we present an analysis of large-scale dynamics of auroral electrons during a substorm, where the results of measurements are in obvious and unambiguous agreement with physical ideas about underlying

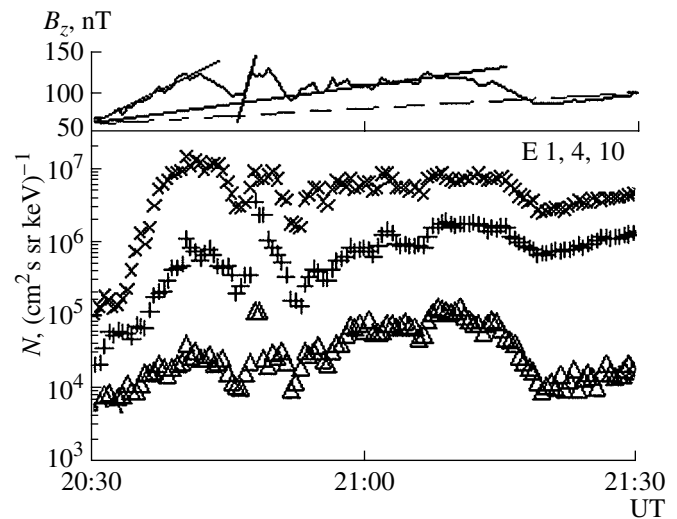


Fig. 2. Synchronism of fast and slow trends in the magnetic field and fluxes of energetic electrons.

ing processes, at least for energetic component. In addition, some conclusions about relationship of dynamics of energetic and low-energy electrons during substorm activations are presented.

2. MEASUREMENTS

In the first part [2] of this paper it was demonstrated that the growth phase of the substorm on March 12, 1991 had begun at about 20:15 or somewhat earlier, at 19:50. The active phase and poleward expansion had begun at 20:26 and 20:30, respectively (here and below, UT is used). The position of the projection of the *CRRES* satellite onto the atmosphere's boundary along the magnetic field line was shown in Fig. 2, while the data of measurements of energetic particles and magnetic field averaged over 30-s intervals are presented in Fig. 8 of the first part of this paper. The Table 1 presents the energy ranges of channels of the sensor of energetic particles and other information about the satellite instrumentation.

The character of time variations recorded by detectors of energetic particles which is shown in the above figure is typical for measurements on geosynchronous satellites during substorms in the longitudinal sector spanned by disturbance. A decline of the particle flux is detected on the growth phase due to radial displacement of the drift shells of 'old' trapped electrons whose flux gradients are directed to the Earth. This decline gives place to a fast intensity growth during dipolarization of the magnetic field. Short bursts of the electron flux are recorded on the background of large-scale variations. These bursts are the sharpest at instants when the satellite turns out to be on field lines of the region of local activation. In our case such local activation on the satellite's longitude was observed at 20:47.

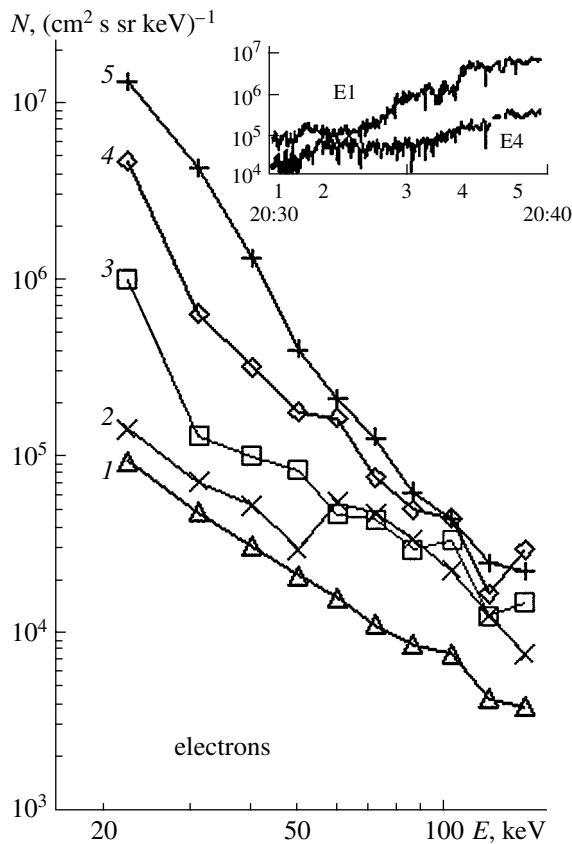


Fig. 3. Dynamics of the energy spectrum of energetic electrons during a large-scale dipolarization. The instants of measurements of the spectra are shown in the inserted panel.

The consolidated plot of electron time variations measured by the LEPA instrument onboard the *CRRES* satellite is presented in Fig. 1. The flux of trapped electrons and field-aligned fluxes are represented by solid and dotted lines, respectively. The bottom panel shows the data of two channels of the EPAS detector of energetic particles. Numerals designate four time intervals of the substorm analyzed in the previous paper. Zero interval corresponds to the last minutes before a breakup, the first and the second intervals are before the beginning of the global dipolarization and during it, respectively. The third interval is the interval of westward shift of WTS and local activation of the meridian of the *CRRES* satellite. Depending on energy, the behavior of electron populations is different. In the interval from 100 eV up to a few keV the flux increases on the stage 0, weakly varies on the 1st stage, and declines during dipolarization. This decline is obviously associated with a general increase of the electron temperature and with the appearance of disturbed fluxes of auroral electrons of the central plasma sheet that represent the second population up to an energy of the order of 20 keV. Here we observe strong variations of intensity with a resulting increase by one–two orders of magnitude to the beginning of dipolarization.

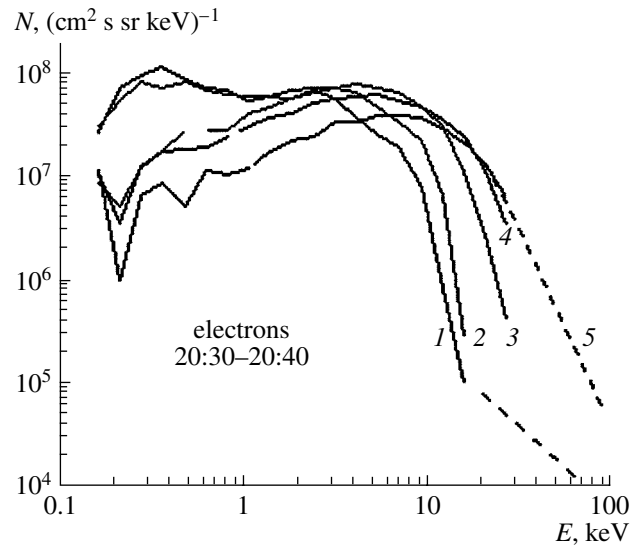


Fig. 4. The same as in Fig. 3, but for CPS electrons.

Finally, the third population above 20 keV constitutes a classical pattern of injection: a growth with the beginning of magnetic field dipolarization and a sharp burst during the local step of the dipolarization.

Pitch-angle distributions of electrons are also different in different energy groups. In the ranges of low and middle energies the stable trapped distribution at the first two stages gives place to the isotropic distribution with overlapped bursts of field-aligned fluxes of electrons with energies below 5 keV.

Let us first consider in more detail the behavior of the second and third populations (i.e., CPS electrons and energetic auroral electrons) during magnetic field dipolarization or large-scale expansion of the substorm.

2.1. Dipolarization

Figure 2 presents the data of measurements of magnetic field and of energetic electrons in several channels; thin straight lines show some trends of growing magnetic field and electron fluxes. The first trend reflects an increase of the electron flux during dipolarization, the second corresponds to local activation, and two long-term trends show the increase of particles and field over the entire active period. In this close connection the magnetic field plays the role of a primary or leading part. Since electrons, unlike ions, are magnetized, the energy density of electrons is relatively small.

Figure 3 shows a sequence of energy spectra of electrons measured by the EPAS detector; the first spectrum reflects the spectrum of trapped electrons of the radiation belt, here there are still no energetic auroral electrons. In the subsequent moments (specified in the insert picture) freshly accelerated electrons appear and the total spectrum is gradually softened. Where these electrons come from is seen in Fig. 4 that presents a

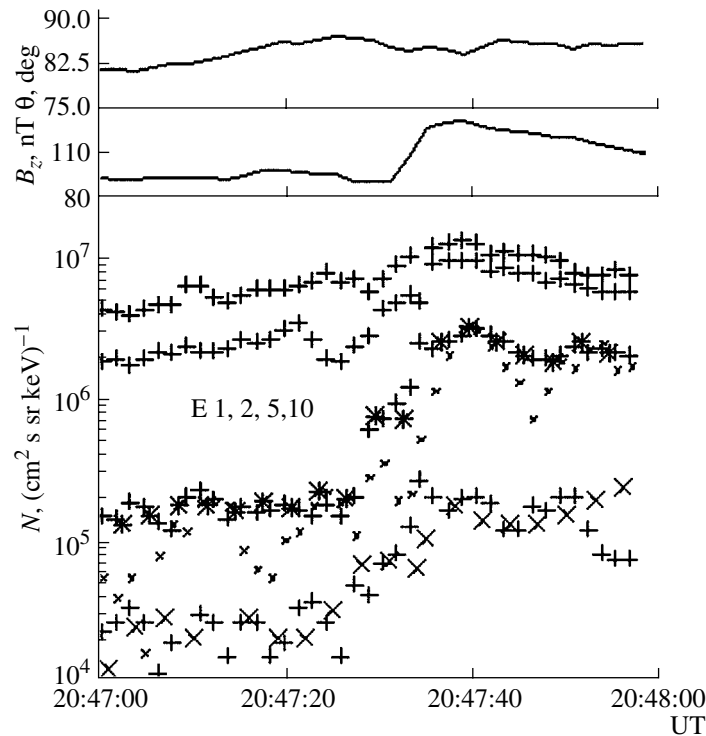


Fig. 5. Time behavior of the magnetic field and particle fluxes during a local activation.

similar plot for soft electrons measured by the LEPA detector. Here also the first curve demonstrates the initial spectrum typical for electrons of the central plasma sheet [3]. The maximum is observed about 0.4 keV

with a power-law character of the spectrum ($N = E^{-k}$), where $k \sim 1$ in the range 1–7 keV and $k \sim 9$ from 7 to 15 keV. In the range of higher energies a transition to a flatter spectrum of trapped electrons of the radiation belt is observed with $k \sim 0.6$. Dashed lines represent the data of measurements of energetic electrons by the EPAS detectors, they well continue the data of the LEPA detector.

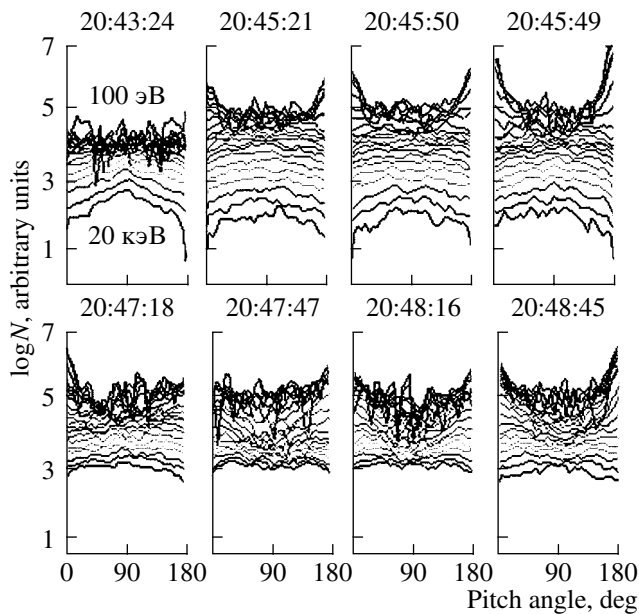


Fig. 6. Pitch-angle distribution of electrons with energies 0.1–20 keV during a local activation.

The next four spectral curves demonstrate the process of fast energizing of the plasma sheet electrons, their transformation (conversion to the population of energetic auroral electrons) takes place during 6–10 min. Every subsequent curve can be obtained from a preceding one by a displacement along the energy axis. In the last curve again, as in the first one, dashed curve continues the spectrum to the region of higher energies, thus demonstrating that spectral curves in Figs. 3 and 4 beautifully match each other.

The process of acceleration of auroral electrons can be unequivocally explained by well the known betatron mechanism. Perpendicular energy of a particle changes proportionally to the ratio of magnetic field strengths at the initial and final points of the trajectory, $W1/W2 = B1/B2$. From 20:32 to 20:37 the electron energy has increased twice, as is seen from the displacement of the falling segment of the spectrum in Fig. 4. At the same time, B_z in the vicinity of *CRRES* has changed approximately from 65 to 110 nT. One can reasonably increase the ratio $B1/B2$ to the desired value merely by taking into account that the convection electric field directed

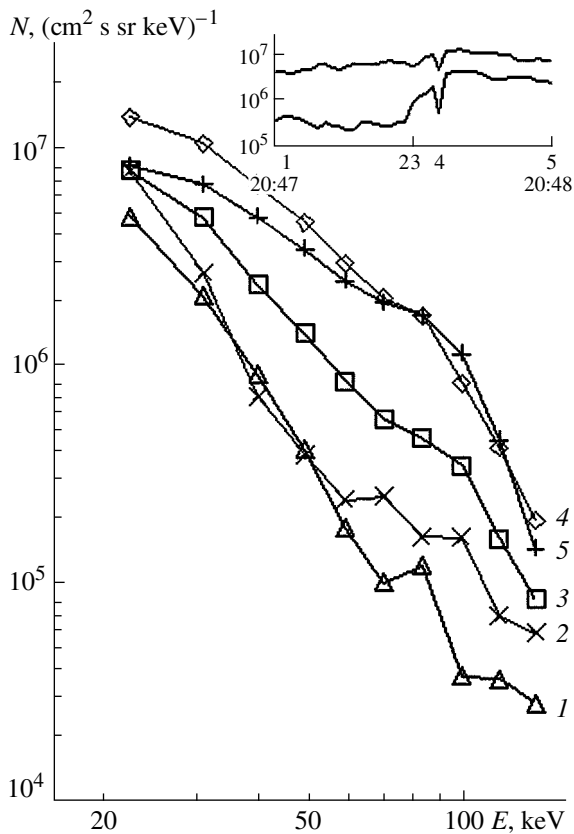


Fig. 7. Dynamics of energy spectra of energetic electrons during a local activation.

to the evening shifts particles to the Earth. The $\mathbf{E} \times \mathbf{B}$ drift from the level of 55 nT located approximately at $0.5 R_E$ from the satellite in the anti-solar direction gives the necessary ratio. Thus, the term “injection” turns out to be justified to some extent, though with an essential correction: injection takes place from the close shells of quasi-trapping region rather than from the tail of the magnetosphere.

2.2. Local Substorm Activation

As was said above, one of substorm activations, near the end of expansion, took place on the meridian of the *CRRES* satellite at 20:43–20:49. As it has been shown by the analysis of magnetic data, this was an activation of the WTS type, i.e., the west front of the sector spanned by the substorm which was orientated in the north-south direction has moved in a jump to the west and was activated in the process of displacement. As a result, both the station Jan Mayen has detected a bay-like disturbance on the near-pole part of bending and disturbances have been observed on the near-equatorial part onto which the field line of *CRRES* location is projected. These disturbances we are going now to describe.

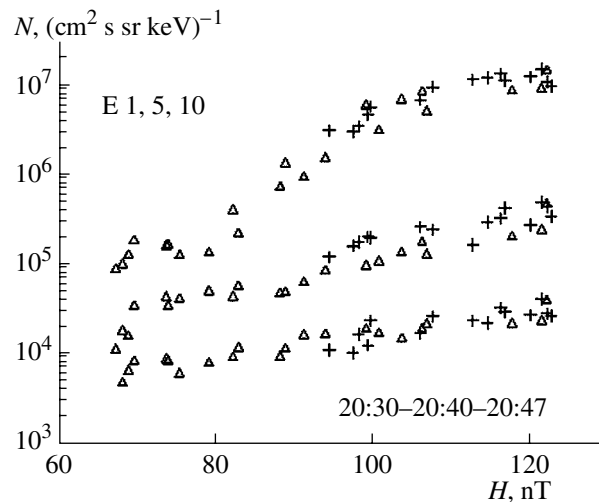


Fig. 8. The electron flux as a function of B_z value on the branches of increase (20:30–20:40) and drop (20:40–20:47) of the intensity.

Let us enumerate basic details of the activation process measured onboard the satellite.

(1) Magnetic field lines are extended to the tail beginning from 20:42. Due to decreasing B_z -component a decrease of the flux of energetic electrons is observed (not shown).

(2) As is seen in Fig. 5, dipolarization begins at 20:47:10. Sharp increases of B_z (from 80 to 130 nT in 5 s) and of the flux of energetic electrons (by an order of magnitude in 10–15 s) occur at 20:47:30–40. This explosive local instability divides the activation in two parts, similar to the first explosive instability of the substorm.

(3) The ions flux begins to increase at the mini-growth phase simultaneously with a decrease of B_z . One can see in Fig. 9 and in paper [1] how the particle energy density increases in the energy ranges 0.1–15 keV and 70–600 keV with approximately equal contribution. At the end of this period the particle energy density exceeds the energy density of magnetic field by a factor of two.

(4) The electric field strength measured onboard the satellite was maximal in this time interval: for all three components of the electrometer the readings are off-scale (> 10 mV/m).

Let us now consider in more detail the dynamics of electrons. Figure 6 demonstrates how the pitch-angle distribution of electrons changes according to measurements on the LEPA detector. Again, we see a difference in the behavior of electrons with energies 0.1–1 keV, 1–5 keV, and 20–100 keV. The first thing that attracts our attention is the appearance of the fluxes of electrons with the lowest energies along field lines at 20:45:20–20:47:00 when magnetic field lines extend into the tail and pressure increases, then this is again observed after interruption at 20:48.45–20:49. This

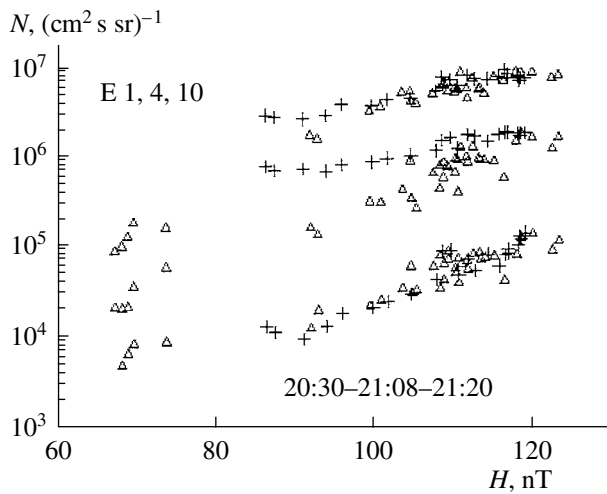


Fig. 9. The same as in Fig. 8 for the long-term trend.

field-aligned flux is seen in Fig. 1 in the channel 0.388 keV.

During the interruption a fast increase of the flux of field-aligned electrons is observed already in the range 1–3 keV, which corresponds to typical energies of electrons causing active forms of aurora. In addition, during the same interval the process of dipolarization takes place, as well as acceleration of energetic electrons 50–100 keV.

Some of pitch-angle distributions presented in Fig. 6 give a symmetrical flux of electrons flowing into the ionosphere and out of it, others are non-symmetrical (in these cases one can speak about the development of a field-aligned current).

Thus, we have the following time sequence: 1) the growth of energy density of ions plus the appearance of field-aligned fluxes of low-energy electrons and then 2) a burst of field-aligned electrons of keV energies, explosive local dipolarization of the magnetic field, acceleration of energetic electrons and a sharp drop of the energy density of particles. Figure 7 presents the spectra of energetic electrons during local activation. One can see a clear distinction from a similar (in the form of representation) pattern of betatron acceleration of electrons during a large-scale dipolarization (Fig. 3). While a successive softening of the energy spectrum was observed there, here we observe predominant acceleration of electrons in a limited energy interval (50–200 keV). In addition, the entire process takes here no more than 10 s and is accompanied by a strong variation of the magnetic field $\partial B/\partial t$, which indicates to acceleration in the inductive magnetic field.

3. DISCUSSION OF RESULTS

The fluxes of electrons and ions play essentially different roles in the processes of substorm activity. Ions govern the variation of the auroral magnetosphere

structure, since they are basic carriers of substorm drift currents. The increasing energy density of ions and spatial inhomogeneity of the plasma pressure establish the conditions for development of the initial explosive instability and for its repetitions in the process of expansion. Electrons have no effect on the large-scale structure of the magnetosphere, but, being accelerated in the process of a substorm, they support the existence of the outer radiation belt and are responsible for a number of substantial process of a substorm, such as auroras, ionospheric absorption of radio waves, auroral electrojet, three-dimensional current wedge of a substorm, X-ray emission, VLF bursts, etc. It is not surprising that almost simultaneous enhancements, injections of electrons and ions turn out to be (upon a detailed consideration) quite different processes in their space-time structure and origin.

For auroral electrons with energies above ten keV the basic factor that determines their dynamics is the magnetic field together with frozenness, drift character of motion, and (though not always) conservation of adiabatic invariants.

The relationship between the magnetic field variation and the increasing intensity of energetic electrons during a relatively slow large-scale dipolarization is determined by two basic processes. One of them is the betatron acceleration that was discussed in the previous section. The resulting energy of a particle is determined by the magnetic field strength at the final point of a particle trajectory; its radial displacement is determined by the $\mathbf{E} \times \mathbf{B}$ drift, where the electric field is the sum of the inductive and convective electric fields. This displacement, as was demonstrated above, was small and limited by the quasi-trapping region.

The second process changing the intensity of electrons detected by the satellite is the radial displacement of drift shells. At the growth phase the drift shells are displaced toward the Earth, and a satellite records a drop of intensity, since the gradient of electron density on the slope of the radiation belt is directed to the Earth. During dipolarization, the reverse motion of the shells of magnetic drift occurs, and one observes an increase of intensity. If the displacement proceeds slowly as compared to the period of drift around the Earth, the third adiabatic invariant is conserved, and the energy of particles remains unchanged.

In Fig. 2 one can observe the magnetic field decrease in two trends after the magnetic field increase, which allows one to compare the character of electron flux dependence on the magnetic field strength at the branches of growth and decline.

Figure 8 shows such a dependence for dipolarization interval 20:30–20:40 and subsequent minutes of B_z decrease for three energy channels of electrons. One can see that the flux of energetic electrons returns back to the previous value upon the field decrease, while in low energies we observe a hysteresis which is an evidence of particle acceleration.

Even more clearly this effect is seen if one considers an example of a long trend embracing the major part of the substorm active phase (Fig. 9). The growth and drop of the magnetic field strength take place from 20:30 to 21:08 and from 21:08 to 21:20, respectively.

In this case energetic electrons are not accelerated, a considerable residual flux of accelerated electrons remains only for energies lower than 90 keV. It seems that there is a superposition of two processes that determine the increasing electron flux during substorm dipolarization, which is illustrated in Fig. 10. Low-energy electrons drift slowly and remain in the active sector over the entire period of substorm expansion, being subject to betatron acceleration. Electrons of high energies should cross the active region almost without acceleration, but the drift shells are displaced: if earlier the satellite detected particles arriving from point “before”, now it is reached by particles from point “after” located closer to the radiation belt maximum. This effect must be determinative for variations of the flux of high-energy electrons recorded by the satellite, and it explains why there is no hysteresis in the plots of Figs. 8 and 9. The upper limit for energy of freshly accelerated auroral electrons in our case was equal to 90 keV, though in stronger substorms it can reach several hundred keV, this follows in particular from balloon measurements of auroral X-ray emission [1].

For electrons with energies higher than 300–700 keV the total energy losses due to pitch-angle scattering become more efficient than acceleration, and geosynchronous satellites record during strong substorms a fast drop of intensity with a subsequent slow (during several days) recovering due to radial diffusion on magnetic impulses [5].

Now passing to an analysis of the results of measurements during local activation let us agree with the fact that it is difficult simultaneously to describe sufficiently clearly the event pattern and to select some new bright result. Enhancements of energetic electrons with intensity growth lasting a few seconds and occurring simultaneously with fast increases of B_z were also observed earlier. The measured energy spectrum cannot be confirmed by anything like a well-substantiated model calculation, since we do not know the geometry of activation and, consequently, the structure of the inductive field. It is impossible having the measurement data at a single point. One can draw the only reliable conclusion about acceleration of electrons precisely by the inductive field; the existence of field-aligned currents and gradients of plasma pressure, and finally, the very variability (a jump) of the magnetic field are sufficient evidence of this.

For low-energy auroral electrons the very fact of detection of field-aligned fluxes is not new, after their observation by McIlwain in 1975 [5] numerous measurements were carried out on various satellites and rockets [7–9]. Onboard the same *CRRES* satellite Abel et al. [10] have discovered considerably diversity of the

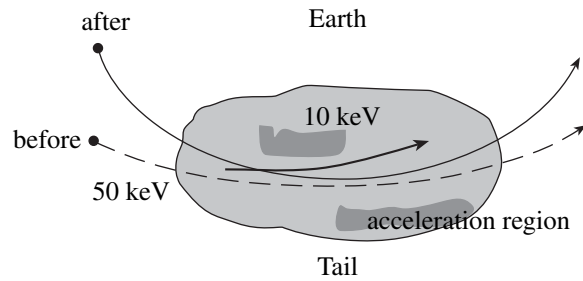


Fig. 10. A scheme of dynamics of electrons during dipolarization.

types of field-aligned electron fluxes both in quiet and in disturbed periods. The complex variable structure of field-aligned precipitation is not surprising, direct confirmation we see in diverse forms of auroras. Quiet arcs, radiate arcs and drapery, active forms of electron auroras—all of them are caused by field-aligned fluxes of electrons with energies from hundreds of eV to ten keV. Probably, only some forms of diffuse auroras and pulsating spots owe their origin to a release of energetic electrons.

Thus, the order and sequence of events before and during the local activation is of interest rather than the mere fact of detection of field-aligned fluxes of electrons. Before the beginning of explosive instability we observe an increase of the fluxes and plasma (ion) pressure simultaneously with the appearance of field-aligned fluxes of low-energy electrons. Then, with an increasing rate the appearance of field-line fluxes of keV electrons is detected, and after that—a burst of energetic electrons, the growth of B_z , and a drop of plasma pressure. Clearly, the fact that this temporal sequence of events is typical should be confirmed again and again, however, it does not contradict the idea of formation of a local dynamic structure of the current wedge type with generation of strong inductive fields whose geometry is similar to the Heikkilä–Pellinen meander [11].

In the first part of our study we drew attention to the fact that enhancements of auroral ions in the beginning of the substorm coincided with aurora bursts and eddy local activations. Since *CRRES* was then located to the west from the epicenter of disturbances, only energetic ions were detected, no field-aligned fluxes are seen, though we are sure they should be present there. The local activation at 20:47 UT is beyond the field of view of ground-based aurora cameras, however, there is no doubt that here also the increase of ion flux was accompanied by an aurora burst. We believe that this regularity (the above coincidence) is an indication in what direction one should search for mechanisms of preparation of the substorm's explosive activation. This is only indication, since because of the slow rotation of the satellite (30 s) there is no necessary time resolution of the pitch-angle distribution of particles and electric field,

and in general, one-point measurement does not allow one to reproduce a particular pattern.

At the same time, the ideas about the decisive role of non-equilibrium plasma pressure in the quasi-trapping region for the substorm development (these ideas are described, in particular, in papers by Antonova [4]) attract more and more attention. The results obtained by us are in line with these ideas. We only emphasize that, speaking about plasma pressure, one should take into account not only the proper CPS plasma, but also essential (and sometimes decisive) contribution of energetic quasi-trapped ions.

CONCLUSIONS

During the substorm on March 12, 1991 we studied the enhancements of auroral electrons in a broad energy range at the time of local activations and large-scale restructuring of the magnetosphere.

(1) At the time of substorm activation the satellite located in the same local field tube records the following sequence of events: the growth of plasma pressure simultaneously with the appearance of field-aligned fluxes of low-energy electrons. Next, the field-aligned fluxes of electrons of keV energies are recorded, then a burst of energetic electrons, an increase of B_z , and a sharp drop of plasma pressure. It is most reasonable to ascribe acceleration of energetic electrons to the inductive electric field. The typical acceleration time is from a few seconds to the first tens of seconds.

(2) Separate localized acts of acceleration of energetic electrons are summarized with large-scale acceleration of the betatron type, caused by increasing magnetic field during the expansion of substorm activity. The typical acceleration time is a few minutes, up to 10–15 min, in this time keV electrons of the CPS turn into the class of quasi-trapped energetic electrons. The large-scale electric field of western direction gives an additional contribution to the acceleration process.

(3) The enhancements of high-energy (> 90–500 keV) electrons are of reversible character and can be explained by the displacement of drift shells to the Earth during the growth phase (and away from the Earth during dipolarization of the magnetic field).

ACKNOWLEDGMENT

The work was supported by the Russian Foundation for Basic Research, grant no. 06-05-64225 (L. Lazutin) and grant DPS-18 (T. Kozelova and B. Kozelov).

REFERENCES

1. Lazutin, L.L., The Structure of the Auroral Magnetosphere and Explosive Processes of Magnetospheric Substorms, in *Fizika okolozemnogo kosmicheskogo prostanstva* (Physics of Near-Earth Space), Apatity: Izd. Kol'skogo nauchnogo tsentra RAN, 2000, vol. 2, pp. 145–192.
2. Lazutin, L.L., Kozelova, T.V., Meredith, N., et al., Studies of the Substorm on March 12, 1991: 1. Structure of Substorm Activity and Auroral Ions, *Kosm. Issled.*, 2007, vol. 45, no. 1., pp. 27–38.
3. Weiss, L.A., Reiff, P.H., Hilmer, R.V., et al., Mapping the Auroral Oval into the Magnetotail Using Dynamics Explorer Plasma Data, *J. Geomagn. Geoelectr.*, 1992, vol. 44, pp. 1121–1144.
4. Antonova, E.E., Equilibrium of Plasma in the Earth's Magnetosphere and Acceleration Processes at High Latitudes, *Doctoral (Phys.-Math.) Dissertation*, Moscow: Skobeltsyn Inst. Nucl. Phys. of Moscow State Univ., 2005.
5. Tverskoi, B.A., *Dinamika radiatsionnykh poyasov Zemli* (Dynamics of the Earth's Radiation Belts), Moscow: Nauka, 1968.
6. McIlwain, C.E., Auroral Beams near the Magnetic Equator, in *The Physics of Hot Plasmas in the Magnetosphere*, Hultqvist, B. and Stenflow, L., Eds., New York: Plenum, 1975, pp. 91–99.
7. Klumpar, D.M., Statistical Distributions of the Auroral Electron Albedo in the Magnetosphere, in *Auroral Plasma Dynamics*, vol. 80 of *Geophys. Monogr. Ser.*, Lysak, R.L., Ed., Washington, D.C.: AGU, 1993, pp. 163–171.
8. Kremser, G., Korth, A., Ullaland, S.L., et al., Field-Aligned Beams of Energetic Electrons (16 keV > E > 80 keV) Observed at Geosynchronous Orbit at Substorm Onsets, *J. Geophys. Res.*, 1988, vol. 93, pp. 14453–14464.
9. Hultqvist, B., Lundin, R., Stasiewicz, K., et al., Simultaneous Observation of Upward Moving Field-Aligned Energetic Electrons and Ions on Auroral Zone Field Lines, *J. Geophys. Res.*, 1988, vol. 86, pp. 9765–9776.
10. Abel, G.A., Fazakerley, A.N., and Johnstone, A.D., The Simultaneous Acceleration and Pitch Angle Scattering of Field-Aligned Electrons Observed by the LEPA on *CRRES*, *J. Geophys. Res.*, 2002, vol. 107, doi:10.1029/2001JA005090.
11. Pellinen, R.J. and Heikkila, W.J., Inductive Electric Fields in the Magnetotail and Their Relation to Auroral and Substorm Phenomena, *Space Sci. Rev.*, 1984, vol. 37, pp. 1–61.